The potential of RCCI concept to meet EURO VI NOx limitation and ultra-low soot emissions in a heavy-duty engine over the whole engine map

Fuel, Volume 159, 1 November 2015, Pages 952–961. http://dx.doi.org/10.1016/j.fuel.2015.07.064

Jesús Benajes, José V. Pastor, Antonio García* and Javier Monsalve-Serrano

CMT - Motores Térmicos, Universitat Politècnica de València, Camino de Vera s/n, 46022 Valencia, Spain

(*) Corresponding author: angarma8@mot.upv.es (Antonio García Martínez)

Abstract

This work investigates the potential of RCCI concept to achieve ultra-low NOx and soot emissions over a wide range of engine speed and loads. For this purpose, a detailed experimental methodology has been defined and applied in a heavy-duty single-cylinder engine fueled with diesel and gasoline. In addition, to assess the influence of the engine compression ratio on RCCI capabilities two different compression ratios, 14.4:1 and 11:1, have been tested.

Results suggest that a low compression ratio allows to fulfill all the self-imposed constraints (maximum cylinder pressure rise rate of 25 bar/CAD, NOx< 0.4 g/kWh and soot*< 0.01 g/kWh) from idle to full load and engine speeds from 900 to 1800 rpm. However, the use of higher compression ratio requires a delayed injection strategy to avoid excessive knocking levels, which results in unacceptable soot emissions at loads higher than 50%, even when gasoline fractions around 90% are used.

Keywords

Reactivity Controlled Compression Ignition; EURO VI; Efficiency; Dual fuel; Engine map

1. Introduction

The stringent regulations introduced around the world to limit the pollutant emissions in internal combustion engines (ICE) present a major challenge for the engine research community. In spite of its efficiency, conventional mixing-controlled diesel combustion in CI diesel engines requires complex and costly exhaust aftertreatment systems to reach the NOx and soot limitations enforced by the current regulations, such as EURO VI. Specifically, the rich local equivalences ratios and the high temperatures achieved during the conventional diesel combustion (CDC) as well as the oxygen availability in the outside of the spray plume results in unacceptable emissions. Additionally aftertreatment systems, which require DPF (to reduce soot emissions) and LNT or SCR (to minimize NOx emissions) can penalize fuel consumption or require a second fluid. Thus, in order to reduce aftertreatment costs and fuel consumption it is necessary to avoid the generation of these pollutants in the focus of the emission, i.e. during the combustion development.

Many new compression ignition combustion strategies have been proposed to simultaneously improve the engine efficiency while reducing the NOx and soot emission levels under the regulation limits [1][2]. The more promising combustion strategies are the well-known low temperature combustion (LTC) strategies. A widely investigated combustion strategy is homogeneous charge compression ignition (HCCI), which produces virtually no soot or NOx emissions while maintaining high efficiency [3][4][5]. However, this combustion process presents new challenges with regard to combustion control and engine stress. Due to the rapid heat release, steep pressure gradients occur so that the process has been limited to use within the partial load range [6]. On this regard, Bessonette et al. [7] suggested that different in-cylinder reactivity is required for the proper HCCI operation under different operating conditions. Specifically, high cetane fuels are required at low load and a low cetane fuel are needed at medium-high load.

With the aim of improving the HCCI shortcomings in terms of controllability and knocking, the use of fuels with lower reactivity than diesel fuel (gasoline-like fuels) under Partially Premixed Combustion (PPC) strategies has been widely investigated [8][9][10][11][12]. The investigations confirmed gasoline PPC as a promising method to control the heat release rate providing a reduction in NOx and soot emissions [13][14]. Thus, by injecting the fuel later in the engine cycle than in HCCI strategy, the air-fuel mixing degree is reduced and therefore higher control on the ignition delay as well as the combustion duration is achieved. Additionally, the use of as a gasoline fuel provides more flexibility to achieve the required extra mixing time at medium-high loads [15]. However, the concept has demonstrated difficulties at low load conditions [16][17] using gasoline with octane number (ON) higher than 90. With the aim of improving the PPC cycle-to-cycle control at low loads using high ON gasolines, PPC spark assisted concept has been studied [18][19]. It has been demonstrated that the spark assistance provides temporal and spatial control over the combustion process [20], however the high local reactivity required between the spark plug electrodes at the start of spark timing and the flame propagation process result in an unacceptable NOx and soot emissions [21]. In this sense, the double injection strategy applied to the PPC spark assisted concept has been confirmed as a suitable strategy to improve the unburned HC and CO emissions, but still do not solve the unacceptable NOx and soot emission levels [22][23].

Recent experimental and simulated studies in a heavy-duty engine demonstrated that Reactivity Controlled Compression Ignition (RCCI) combustion is a more promising LTC technique than HCCI and PPC [24][25]. RCCI concept is a partially premixed combustion strategy based on dual-fuel operation. To delivery both fuels separate injection systems for the low reactivity and high reactivity fuel are used, being port fuel injected (PFI) and direct injected (DI) respectively. Therefore, a flexible operation over a wide range is possible by modifying both, the low reactivity fuel percentage in the blend [26] and the direct injection timing [27]. The variation of these engine settings provides the required in-cylinder equivalence ratio and reactivity (i.e. octane number) stratification. Thus, previous studies in a heavy-duty engine at fixed engine speed of 1300 rpm and 1200 rpm, evaluated RCCI concept from low to high load concluding that RCCI provides very low NOx and soot compared to the reference CDC cases. In addition, a benefit in fuel consumption from low to medium load compared to CDC was also appreciated [28]. In this sense, it was confirmed that RCCI combustion process converts greater percentage of the recovered heat transfer energy into useful work than in CDC operation [29]. Thus, it was also demonstrated that the combination of different strategies to reduce heat transfer losses, such as the use of an optimized piston bowl geometry without piston cooling, allows to reach gross indicated thermal efficiencies near 60% [30]. In spite of the benefits of RCCI concept in terms of fuel consumption, a worse combustion efficiency than CDC was observed, with values around 97% at low load conditions. In this regard, an experimental investigation combined with computational modelling [31], demonstrated that it is possible to improve the low load combustion efficiency to values above 98% by combining the effects of in-cylinder gas temperature and oxygen concentration respectively with the in-cylinder fuel blending ratio.

The main objective of the present work is to examine the potential of RCCI concept in a wider range of engine speed and loads in a heavy-duty engine. For this purpose, a detailed experimental methodology has been defined to ensure stable RCCI operating conditions while fulfilling three self-imposed constraints (maximum cylinder pressure rise rate of 25 bar/CAD, NOx< 0.4 g/kWh and soot*< 0.01 g/kWh). In addition, to assess the influence of the engine compression ratio on RCCI capabilities two different compression ratios, 14.4:1 and 11:1, have been tested.

2. Experimental Facilities and Processing Tools

2.1. Test cell and engine description

A single cylinder, heavy-duty diesel engine representative of commercial truck engine, has been used for all experiments in this study. The major difference to the standard unit production is the hydraulic VVA system, which conferred great flexibility during the research. In particular, the valve timing, duration and lift can be electronically controlled for each valve during the engine tests. Detailed specifications of the engine are given in Table 1.

The engine was installed in a fully instrumented test cell, with all the auxiliary facilities required for its operation and control, as it is illustrated in Figure 1.

Moreover, to achieve stable intake air conditions, a screw compressor supplied the required boost pressure before passing through an air dryer. The air pressure was adjusted in the intake settling chamber, while the intake temperature was controlled in the intake manifold after mixing with the EGR flow. The exhaust backpressure produced by the turbine in the real engine was replicated by means of a valve placed in the exhaust system, controlling the pressure in the exhaust settling chamber. Low pressure EGR was produced taking exhaust gases from the exhaust settling chamber. Then, once it was filtered by a DPF, its temperature was reduced passing through a heat exchanger. After that, condensate water and other substances were separated from the gas by means of a centrifugal filter, and the resulting flow was passed through a secondary filter. Furthermore, a roots-type supercharger was used in order to provide the external EGR mass flow rate desired. With the aim of lowering the gas temperature increase caused by the supercharger, a second heat exchanger was used before the arrival of the EGR gases to a settling chamber equipped with an electric heater. It was then introduced into the intake pipe, closing the external EGR loop. The temperature regulation was performed upon the EGR-fresh air mixture, by means of a temperature sensor in the intake manifold. Finally, the exact EGR rate was controlled by means of a valve between the EGR settling chamber and the intake pipe. The determination of the EGR rate was carried out using the experimental measurement of intake and exhaust CO_2 concentration. The concentrations of NOx, CO, unburned HC, intake and exhaust CO_2, and O_2 were analyzed with a five gas Horiba MEXA-7100 DEGR analyzer bench by averaging 40 seconds after attaining steady state operation. Smoke emission were measured with an AVL 415S Smoke Meter and averaged between three samples of a 1 liter volume each with paper-saving mode off, providing results directly in FSN (Filter Smoke Number) units. A limitation to using a smoke meter based on opacity is that it may not accurately account for condensable organic hydrocarbons in the PM, which have been shown to be the primary PM mode with RCCI [32]. Thus, measurements of FSN were converted into estimated specific soot* emissions (g/kWh) by means of the factory AVL calibration (mg/m^3) and considering the volumetric exhaust gas flow, but it should be noted that estimated soot* may differ to the real soot amount. According to previous studies, the relationship between FSN and real PM for RCCI operation should be examined further.

2.2. Fuels and delivery

Commercially available diesel and 98 ON gasoline fuels were selected as high and low reactivity fuels, respectively. Their main properties related with auto-ignition are listed in Table 2.

To enable RCCI operation the engine was equipped with a double injection system, one for each different fuel used, as it is shown in the scheme of Figure 2. This injection hardware enables to vary the in-cylinder fuel blending ratio and fuel mixture properties according to the engine operating conditions.

To inject the diesel fuel, the engine was equipped with a common-rail flexible injection hardware which is able to perform up to five injections per cycle. The main characteristic of this hardware is its capability to amplify common-rail fuel pressure for one of the injections by means of a hydraulic piston directly installed inside the injector. The main characteristics of the injector and nozzle used are depicted in Table 3.

Concerning the gasoline injection, an additional fuel circuit was in-house built with a reservoir, a fuel filter, a fuel meter, an electrically driven pump, a heat exchanger and a commercially available port fuel injector (PFI). This injector was located at the intake manifold and was specified to be able to place all the gasoline fuel into the cylinder during the intake stroke. The gasoline injection timing was fixed at 10 CAD after the IVO to allow the fuel to flow along the distance of 160 mm from the PFI location up to the intake valves during the intake stroke. The objective was to avoid fuel pooling over the intake duct surface and the undesirable variability in the mixture formation caused by this phenomenon. The main characteristics of the gasoline injector are depicted in Table 4.

2.3. Analysis of in-cylinder pressure signal

The combustion analysis was performed with an in-house one-zone model named CALMEC, which is fully described in the literature [33]. This combustion diagnosis tool uses the in-cylinder pressure signal as its main input. The in-cylinder pressure was measured with a Kistler 61215C pressure transducer coupled with a Kistler 5011B10 charge amplifier. A shaft encoder with 1800 pulses per revolution was used, which supplies a resolution of 0.2 CAD. The pressure traces from 150 consecutive engine cycles were recorded in order to compensate the cycle-to-cycle variation during engine operation. Later, each individual cycle pressure data was smoothed using a Fourier series low-pass filter with a variable cutoff frequency depending on engine speed [34][35]. Once filtered, the collected cycles were ensemble averaged to yield a representative cylinder pressure trace, which was used to perform the analysis. Then, the first law of thermodynamics was applied between IVC and EVO, considering the combustion chamber as an open system because of blow-by and fuel injection. The ideal gas equation of state was used to calculate the mean gas temperature in the chamber. Along with these two basic equations, several sub-models were used to calculate instantaneous volume and heat transfer, among other things [36]. The main result of the model was the Rate of Heat Release (RoHR). Information related to each cycle can be obtained, such as the IMEP. Start of combustion (SOC) was defined as the crank angle position in which the RoHR slope begins to rise due to combustion and combustion phasing is defined as the crank angle position of 50% fuel mass fraction burned (CA50).

3. Results and discussion

3.1. Experimental procedure

As explained in the introduction section, a mandatory constraint in this study is to ensure NOx levels under EURO VI limit and ultra-low soot emissions. In addition, from the engine’s mechanical integrity point of view, a restricted cylinder pressure rise rate is also necessary. Figure 3 and Figure 4 show a scheme of the experimental procedure with the three steps in order to reach the three imposed constraints over a wide range of engine speed and loads.

The first step is aimed at finding the potential engine settings allowing stable RCCI operation at the desired engine load. As literature demonstrates [37], the more effective control parameters over RCCI combustion are the diesel injection timing and the in-cylinder fuel blending ratio (diesel to gasoline ratio in the blend). In this sense, for fixed intake charge properties, the single or the combined modification of these parameters enables the modulation of the combustion development to achieve a stable combustion with a desired combustion phasing. Figure 3 illustrates that, starting from the reference CDC case at low load, the stable RCCI conditions at desired load can be reached by gradually increasing the gasoline fraction (defined in terms of mass in this work) and advancing diesel SOI. Both actions favor low soot emission levels, which is one of the objectives of the global procedure. Nevertheless, it is interesting to remark that the maximum gasoline fraction is limited to ensure stable conditions (COV_{IMEP}< 4%) and the SOI advance is also limited to avoid excessive knocking (PRR_{max}< 25 bar/CAD). The CDC settings are the ones used by the authors in the reference test, which is measured every day before starting the experimental batch of tests. These settings are not relevant for the development of the global procedure.

In the second step, a loop to reach EURO VI limits in terms of NOx together with soot* levels below 0.01 g/kWh is proposed. In this case, additionally to the diesel SOI and gasoline fraction, the EGR rate was also considered as key variable to reach the goal. It is interesting to remark that no explicit restrictions in terms of CO and HC emissions are imposed in this step, but the limitation introduced in the coefficient of variation of the IMEP (COV_{IMEP} <4%) is aimed to avoid misfire conditions (with unacceptable HC and CO). As a result of this second step, a NOx and soot* compliant engine operating point but not optimized in terms of HC and CO emissions is achieved (noted as *potential setting* in the figure).

Finally, an *optimization* step (referred as *fine tuning* in the scheme of Figure 4) was done. The objective of this final step is to minimize HC and CO emissions as well as to improve the fuel consumption while maintaining NOx< 0.4 g/kWh and soot*< 0.01 g/kWh. In this case, the EGR rate and diesel SOI were found as the key engine variables. Figure 5 illustrates the effect of the EGR rate on RCCI engine-out emissions at high load and 1200 rpm. In this case, the operating conditions obtained at the end of the second step (denoted as *initial point* in the figure) resulted in NOx and soot* levels considerably lower than the limits proposed, with an excessive CO and HC emissions. As expected, the EGR reduction provides an improvement of around 45% and 76% in HC and CO emissions, respectively. Moreover, soot* emissions are decreased as EGR is reduced due to the enhancement of its oxidation process, and NOx emissions remains below the limit of 0.4 g/kWh. Further reductions in the EGR rate only will cause the non-compliance in terms of NOx emissions. From the figure, the reduction in HC and CO emissions is clearly linked to the enhancement in the second combustion stage, when the majority of gasoline is consumed [31]. Thus, a notable increase in the maximum RoHR peak is appreciated in this second stage, while in the first one is progressively reduced. It is also interesting to remark that combustion phasing remains almost unchanged with the EGR modification (only a 0.6 CAD variation between the extremes was appreciated).

On the other hand, Figure 6 shows the potential of combining both effects (EGR rate and diesel SOI modification) in order to reduce HC and CO emissions while maintaining a desired combustion phasing. It contributes not only to reduce the emission levels, but also to improve the fuel consumption (BSFC). As seen in the figure, the first advance in diesel SOI (from -8 CAD to -11 CAD ATDC) results in a notable improvement in BSFC. This improvement is related with the better combustion phasing achieved (CA50 moved from 11.1 CAD to 7.5 CAD ATDC), which allows enhancing the fuel to work efficiency. In addition, a great reduction in HC and CO emissions is observed. In this sense, as the combustion development is shifted to higher pressure and temperature conditions, the late soft burn (which causes the majority of unburned products) is avoided. Once a desired combustion phasing (CA50) is reached, the combined modification of the EGR rate and diesel SOI allows to modulate the combustion development in order to search slight improvements in BSFC and emissions. Comparing the RoHR traces of SOI -13 and -32 CAD is possible to appreciate how the combustion shape changes from a two staged to a one stage heat release. The advance in diesel SOI without the additional modification of other engine settings results in an over-dilution of the diesel fuel injected, and then lower ERG rate is needed to maintain a stable combustion with a desired CA50. Thus, focusing on the RoHR shape of SOI -32 CAD, it is clear that almost the whole combustion development takes place after TDC. In addition, the improved in-cylinder reactivity, due to the EGR reduction, results in a higher RoHR peak. Both factors lead to a reduction of 3.5% in BSFC. Also of note is that CO and HC emissions are not strongly affected with this strategy. It is believed that once certain emission levels are achieved, the emissions are mainly governed by geometric factors such as squish flow and crevices and not by the engine settings [29].

3.2. RCCI engine mapping results

This section presents a summary of the trends obtained following the experimental procedure described above. It is interesting to remark that only the results that fulfill all the imposed constraints are represented. In order to perform the maps, different engine loads from idle to full load and engine speeds from 900 to 1800 rpm have been tested.

3.2.1. Compression ratio of 14.4:1

In a first approach, the nominal compression ratio of 14.4:1 was tested. Figure 7 represents different key parameters for the RCCI combustion analysis as a function of the engine speed and load. The dashed lines across the figure denote the BMEP values of 10%, 25%, 50%, 75% and 100% load at 1200 rpm for the CDC cases using the baseline engine settings. In addition, the specific RCCI measured points are highlighted with black dots in the maps.

In this the figure, it can be observed that RCCI engine mapping was only possible up to 50% load (load referred to CDC at 1200 rpm) whatever the engine speed. In this regard, it is remarkable that neither the excessive knocking level nor the combustion stability are limiting factors for extending the RCCI mode to higher values of BMEP. As observed, the experimental procedure defined to reach stable RCCI conditions (Figure 3) ensures maximum PRR values well below 25 bar/CAD in all the operating points, with higher values as BMEP is increased and engine speed is reduced. In this case, the low engine speed allows higher time to burn and enhances the combustion process, which is confirmed looking the CO and HC trends in Figure 8. Hence, the more fuel mass burned leads to higher knocking levels. On the other hand, stable combustion is attained in all the tests with COV_{IMEP} values only slightly higher than 4% at 1800 rpm and idle conditions. Also worth noting is that the comparison of these two parameters confirm its inverse relationship, with more stable combustion (lower COV_{IMEP}) as PRR is increased.

From the gasoline fraction map analysis, is observed that the maximum GF achievable while fulfilling the combustion stability criteria at low load was around 37%. In addition, for a given engine load, the GF was maintained as the engine speed varied without knocking or stability problems. Thus, the higher GF region is found at 25% load, where a maximum GF of 89.9% at 1800 rpm was set. Finally, focusing on gross indicated efficiency (GIE) trend, it is clear that it increases as engine speed increases. In addition, the higher value found in this specific study was 47.2% at 1800 rpm and 25% load, which corresponds to the test with the highest GF. The trend of GIE as a function of the engine load shows a parabolic behavior, with maximum values between 25% and 50% load, which also correspond with the higher GF levels in the map. Hence, it is confirmed that to achieve high efficiency while maintaining low NOx and soot* emissions, the larger portion of the energy should come from the low reactivity fuel.

Figure 8 represents the engine-out emissions in a similar way as in previous figure. As explained in the experimental procedure, soot* emission levels were a key experimental constraint with a imposed limit of 0.01 g/kWh that could be achieved across the whole engine map. As seen from the figure, at 50%

load soot* levels are very close to the limit (mainly at 1200 rpm). It was confirmed that further increase in load (i.e. in fuel mass) pushed the soot* levels over the maximum allowed value, even with GF greater than 90%. These high soot* levels are consequence of the required delay in diesel SOI to avoid excessive PRR as load is increased (Figure 3). As a consequence, the mixing time for diesel injection is reduced and the mixture distribution at SOC becomes richer, which promotes the soot formation. This fact limits the RCCI engine map to 50% load with the nominal compression ratio.

Regarding NOx emissions, it is worthy to note that all the values are below EURO VI limitation (0.4 g/kWh). In addition, the trend obtained differs notably to the one observed in the other pollutant emissions. In this case, a greater dependency on the engine speed is found with lower emission levels for the 900 and 1500 rpm operating points. Additionally, a rise in NOx levels is observed as load is increased. This fact is explained due to the enhancement in the combustion development (higher stability and low HC and CO).

HC and CO emissions were found to decrease as BMEP increased. As expected, the lower HC and CO emissions are located in the region of the map with great combustion stability and also high PRR. Inside this region, the slight differences in the emission values are the result of variations in diesel SOI, stability and GF. Thus, the engine operating condition with the best balance in terms of HC and CO emissions achieved in this specific study was found at 1500 rpm and 50% load, with 3.9 g/kWh and 4.4 g/kWh respectively.

3.2.2. Compression ratio of 11:1

In order to explore the potential of RCCI concept at higher loads, an effective compression ratio of 11:1 was set by means of advancing the intake valves closing event (early Miller cycle).

Figure 9 shows the same parameters as in the previous section, but for compression ratio of 11:1. The figure shows how with this lower compression ratio, the RCCI operation can be extended towards high BMEP, and almost up to full load at 1200 rpm. In addition, it is found that the trends in COV_{IMEP} and PRR are the same found with high CR, with higher PRR and combustion stability as BMEP is increased and engine speed is reduced. Also of note is that at 50% load, slightly higher maximum PRR values than in the case of CR 14.4:1 were obtained. The lower CR allows to advance the diesel SOI to minimize soot formation, which implies slightly higher maximum PRR than the same operating condition at CR 14.4:1. Consequently, the maximum PRR registered in this study was 25.1 bar/CAD at 1200 rpm and 96% load.

On the other hand, the maximum COV_{IMEP} values are slightly lower than with CR 14.4:1 and the minimum values are lower too, which denotes that the combination of the settings proposed with the lowered CR provide higher combustion stability in the whole engine map.

Focusing on the gasoline fraction effect, three different areas are identified. At idle conditions, in which a higher amount of diesel fuel was needed to maintain stable operation, the GF varies from 35% (at high engine speed) to 65% (at low engine speed), since the more unstable conditions at 1800 rpm require higher diesel fuel amount in the blend. In a region between 25% and 75% load, the GF varies from 70% to 78% with peaks of 88% at 1200 rpm. Finally, at high load a peninsula with lower GF than at medium load is appreciated. This fact is consequence of a technological limitation. In particular, the higher boost pressure required at high load restricts the injection rate of the gasoline injector, and an increase in diesel injection is needed to reach the target load. Finally, gross indicated efficiency increases as engine speed and load increase. The highest value found was 48.2% at 1200 rpm and 96% load. It is interesting to remark that a similar value is obtained at 1500 rpm and 85% load.

As far as engine-out emissions, Figure 10 shows that soot* levels remain under the imposed value in the whole engine map. The peninsula with higher soot levels corresponds to the peninsula of the limited GF at high load. In this sense, since a large total fuel mass has to be supplied to the engine at this operating condition, a GF around 75% still implies high diesel injected mass, which enhances the soot formation. The NOx emissions trend suggest a stronger dependency on engine speed than on engine load. Only at 1800 rpm a clear change in NOx emissions levels is observed as a function of the engine load. At this engine speed, a region with values near the limit is observed between 10% and 25% load, with a maximum NOx level of 0.39 g/kWh. This fact is well related with the low GF used in this case (35%). In addition, it is demonstrated that all the values remain below the EURO VI limitation.

Finally, as found with CR 14.4:1, HC and CO emissions levels were notably reduced as BMEP increased. The lower HC and CO emissions are also located in the zone of the map with the greater combustion stability and PRR. Specifically, values of HC=0.17 g/kWh and CO=1.75 g/kWh were attained at 1500 rpm and 85% load. This represents a 95% improvement in HC and 60.2% in CO versus the best balanced operating point in terms of these emissions at CR 14.4:1.

In order to compare directly the effect of compression ratio, Figure 11 shows the engine-out emissions, PRR and GIE versus engine load for both compression ratios at constant engine speed of 1200 rpm. The main findings previously described are also confirmed in this figure. Lowered compression ratio allows achieving the constraints proposed over the whole engine load sweep, while nominal compression ratio exceeds the soot* limitation from medium load.

4. Conclusions

In the present study, the potential of RCCI concept to reach EURO VI NOx levels and ultra-low soot emissions in a heavy-duty engine over the whole engine map has been demonstrated. For this, a detailed experimental methodology has been defined and applied to obtain maps of the engine-out emissions and other different parameters. Moreover, two different compression ratios, 14.4:1 and 11:1, have been evaluated.

From the experimental engine procedure, it is found that the key variables to reach stable RCCI operation are the diesel injection timing and the in-cylinder fuel blending ratio. The modification of both variables allows to modulate the combustion pashing while maintaining a certain pressure rise rate with a high gasoline fraction in the blend. In a second step, aimed at introducing the potential RCCI engine operating points under the EURO VI NOx and soot* limitations, the exhaust gas recirculation (EGR) rate was also considered as key variable. In addition, the limitation in the COV of IMEP introduced in this step allows to control the CO and HC emission levels. Finally, an *optimization* step is needed to minimize CO and HC emissions.

It should be noted that the results presented here have not been rigorously optimized and it is expected that different combinations of injection parameters, EGR levels, and gasoline percentages may yield similar results.

Following the defined experimental procedure, the ability of RCCI concept to be mapped has been demonstrated. The key conclusions from the analysis of the different results presented in the maps are summarized as follows:

- The methodology proposed ensures to achieve the imposed limitations of maximum PRR and COV_{IMEP} without limiting the upper portion of the RCCI engine map.
- The high soot* levels, consequence of the progressive delay in diesel SOI to avoid excessive PRR as load is increased, limited the RCCI engine map to 50% load at nominal CR of 14.4:1. This restriction was solved by lowering the CR to 11:1.

- NOx emissions trends showed a stronger dependency on engine speed than the other pollutant emissions. In this case, all the values are below EURO VI limitation for both compression ratios.
- Gross indicated efficiency increased with engine speed and load. In addition, the regions of maximum GIE values in the map correspond with the higher GF levels. A 48.2% peak of GIE at 1200 rpm and 96% load was found with CR 11:1.
- For both compression ratios, HC and CO emissions were reduced as BMEP increased. In addition, the lower HC and CO emissions were located in the region of the map with great combustion stability and PRR. The comparison of the best balanced operating conditions for both CR values suggested that the extension in load range achieved with CR 11:1 results also in a great improvement in both emissions.

References

[1]Yanagihara H, Sato Y, Minuta J. A simultaneous reduction in NOx and soot in diesel engines under a new combustion system (Uniform Bulky Combustion System e UNIBUS), in: 17th International Vienna Motor Symposium, pp. 303-314, 1996.

[2]Wu H-W, Wang R-H, Ou D-J, Chen Y-C, Chen T-Y. Reduction of smoke and nitrogen oxides of a partial HCCI engine using premixed gasoline and ethanol with air. Applied Energy, Vol. 88, pp 3882-3890, 2011.

[3]Maurya R K, Agarwal A K. Experimental study of combustion and emission characteristics of ethanol fuelled port injected homogeneous charge compression ignition (HCCI) combustion engine. Applied Energy, Vol. 88, pp 1169-1180, 2011.

[4]Lu X, Han D, Huang Z. Fuel design and management for the control of advanced compression-ignition combustion modes. Progress in Energy and Combustion Science, 37, 2011:741-783.

[5]Mingfa Y, Zhaolei Z, Haifeng L. Progress and recent trends in homogeneous charge compression ignition (HCCI) engines. Progress in Energy and Combustion Science 35 (5) (October 2009) 398-437.

[6]Cerit M, Soyhan H S. Thermal analysis of a combustion chamber surrounded by deposits in an HCCI engine. Applied Thermal Engineering 50 (1) (2013) 81-88.

[7]Bessonette P W, Schleyer C H, Duffy K P, Hardy W L, Liechty M P. Effects of fuel property changes on heavy-duty HCCI combustion. SAE paper 2007-01-0191, 2007.

[8]Singh A P, Agarwal A K. Combustion characteristics of diesel HCCI engine: an experimental investigation using external mixture formation technique. Appl Energy 2012. Volume 99, November 2012, Pages 116-125

[9]Law D, Kemp D, Allen J, Kirkpatrick G, Copland T. Controlled combustion in an IC-engine with a fully variable valve train. SAE paper 2001-01-0251; 2001.

[10]Agrell F, Ångström H-E, Eriksson B, Wikander J, Linderyd J. Integrated simulation and engine test of closed loop HCCI control by aid of variable valve timings. SAE paper 2003-01-0748; 2003.

[11]Haraldsson G, Tunestål P, Johansson B, Hyvönen J. HCCI combustion phasing in a multi cylinder engine using variable compression ratio. SAE paper 2002-01-2858; 2002.

[12]Maurya R K, Agarwal A K. Experimental investigation on the effect of intake air temperature and air–fuel ratio on cycle-to-cycle variations of HCCI combustion and performance parameters. Applied Energy, Vol. 88, pp 1153-1163, 2011.

[13]Kalghatgi G T. Auto-ignition quality of practical fuels and implications for fuel requirements of future SI and HCCI engines. SAE paper 2005-01-0239, 2005.

[14]Kalghatgi G, Risberg P, Angstrom H. Advantages of fuels with high resistance to autoignition in late-injection, low-temperature, compression ignition combustion. SAE Trans., 2006, 115(4), 623–634.

[15]Lewander C M, Johansson B, Tunestal P. Extending the Operating Region of Multi-Cylinder Partially Premixed Combustion using High Octane Number Fuel. SAE Paper 2011-01-1394; 2011.

[16]Liu H, Yao M, Zhang B, Zheng Z. Effects of inlet pressure and octane numbers on combustion and emissions of a homogeneous charge compression ignition (HCCI) engine. Energy and Fuels, 2008, 22(4), 2207–2215.

[17]Christensen M, Hultqvist A, Johansson B. Demonstrating the multi-fuel capability of a homogeneous charge compression ignition engine with variable compression ratio. SAE paper 1999-01-3679, 1999.

[18]Benajes J, García A, Domenech V, Durrett R. An investigation of partially premixed compression ignition combustion using gasoline and spark assistance. Applied Thermal Engineering, Volume 52, Issue 2, 15 April 2013, Pages 468-477.

[19]Pastor JV, García-Oliver JM, García A, Micó C, Durrett R. A spectroscopy study of gasoline partially 365 premixed compression ignition spark assisted combustion. Applied Energy 2013;104:568–75. 366.

[20]Benajes J, García A, Tormos B, Monsalve-Serrano J. Impact of Spark Assistance and Multiple Injections on Gasoline PPC Light Load. SAE Int. J. Engines 7(4):2014, doi:10.4271/2014-01-2669.
[21]Desantes JM, Payri R, García A, Monsalve Serrano J. Evaluation of Emissions and Performances from Partially Premixed Compression Ignition Combustion using Gasoline and Spark Assistance. SAE Technical Paper 2013-01-1664, 2013, doi:10.4271/2013-01-1664.
[22]Benajes J, García A, Molina S, Monsalve-Serrano J, Durrett R. Conceptual model description of the double injection strategy applied to the gasoline partially premixed compression ignition combustion concept with spark assistance. Applied Energy, Volume 129, 15 September 2014, Pages 1-9.
[23]Benajes J, García A, Molina S, Monsalve-Serrano J, Durrett R. Performance and engine-out emissions evaluation of the double injection strategy applied to the gasoline partially premixed compression ignition spark assisted combustion concept. Applied Energy, Volume 134, 1 December 2014, Pages 90-101.
[24]Kokjohn S, Hanson R, Splitter D, Reitz R. Experiments and Modeling of Dual-Fuel HCCI and PCCI Combustion Using In-Cylinder Fuel Blending. SAE Int. J. Engines 2(2):24-39, 2010, doi:10.4271/2009-01-2647.
[25]Splitter D A, Wissink M L, Hendricks T L, Ghandhi J B, Reitz R D. Comparison of RCCI, HCCI, and CDC Operation from Low to Full Load, THIESEL 2012 Conference on Thermo- and Fluid Dynamic Processes in Direct Injection Engines, 2012.
[26] Benajes J, Molina S, García A, Monsalve-Serrano J. Effects of Low Reactivity Fuel Characteristics and Blending ratio on Low Load RCCI Performance and Emissions in a Heavy-Duty Diesel Engine. Energy, 2015, doi:10.1016/j.energy.2015.06.088.
[27] Benajes J, Molina S, García A, Monsalve-Serrano J. Effects of Direct injection timing and Blending Ratio on RCCI combustion with different Low Reactivity Fuels. Energy Conversion and Management, Volume 99, 15 July 2015, Pages 193-209.
[28]Molina S, García A, Pastor JM, Belarte E, Balloul I.Operating range extension of RCCI combustion concept from low to full load in a heavy-duty engine. Applied Energy, Volume 143, 1 April 2015, Pages 211-227

[29]Kokjohn S L, Hanson R M, Splitter D A, Reitz R D. Fuel reactivity controlled compression ignition (RCCI): a pathway to controlled high-efficiency clean combustion, International Journal of Engine Research, 2011.

[30]Splitter D, Wissink M, DelVescovo D, Reitz R. RCCI Engine Operation Towards 60% Thermal Efficiency. SAE Technical Paper 2013-01-0279, 2013, doi:10.4271/2013-01-0279.

[31]Desantes JM, Benajes J, García A, Monsalve-Serrano J. The Role of the In-Cylinder Gas Temperature and Oxygen Concentration over Low Load RCCI Combustion Efficiency. Energy, http://dx.doi.org/10.1016/j.energy.2014.10.080.

[32] Prikhodko V, Curran S, Barone T, Lewis S, Storey J, Cho K, et al. Emission Characteristics of a Diesel Engine Operating with In-Cylinder Gasoline and Diesel Fuel Blending. SAE Int. J. Fuels Lubr. 3(2):946-955, 2010, doi:10.4271/2010-01-2266.

[33]Payri F, Olmeda P, Martín J, García A. A complete 0D thermodynamic predictive model for direct injection diesel engines. Applied Energy, Volume 88, Issue 12, December 2011, Pages 4632-4641.

[34] Payri F, Olmeda P, Guardiola C, Martín J. Adaptive determination of cut-off frequencies for filtering the in-cylinder pressure in diesel engines combustion analysis. Applied Thermal Engineering 31 (2011) 2869-2876.

[35] Payri F, Luján JM, Martín J, Abbad A. Digital signal processing of in-cylinder pressure for combustion diagnosis of internal combustion engines. Mechanical Systems and Signal Processing 24 (2010) 1767-1784.

[36]Payri F, Olmeda P, Martin J, Carreño R. A New Tool to Perform Global Energy Balances in DI Diesel Engines. SAE Int. J. Engines 7(1):2014, doi:10.4271/2014-01-0665.

[37]Splitter D, Hanson R, Kokjohn S, Wissink M, et al. Injection Effects in Low Load RCCI Dual-Fuel Combustion. SAE Technical Paper 2011-24-0047, 2011, doi:10.4271/2011-24-0047.

Abbreviations

ATDC: After Top Dead Center

BMEP: Break Mean Effective Pressure

BSFC: Break Specific Fuel Consumption

CA50: Crank Angle at 50% mass fraction burned

CDC: Convention Diesel Combustion

COV: Coefficient of Variation

CI: Compression Ignition

DI: Direct Injection

DPF: Diesel Particulate Filter

EVC: Exhaust Valve Closing

EVO: Exhaust Valve Opening

FSN: Filter Smoke Number

GF: Gasoline Fraction

GIE: Gross Indicated Efficiency

HCCI: Homogeneous Charge Compression Ignition

IMEP: Indicated Mean Effective Pressure

IVC: Intake Valve Close

IVO: Intake Valve Open

LNT: Lean NOx Trap

LTC: Low Temperature Combustion

MON: Motor Octane Number

ON: Octane Number

PM: Particulate Matter

PFI: Port Fuel Injection

PPC: Partially Premixed Charge

PRR: Pressure Rise Rate

RCCI: Reactivity Controlled Compression Ignition

RON: Research Octane Number

RoHR: Rate of Heat Release

SCR: Selective Catalytic Reduction

SOC: Start of Combustion

SOI: Start of Injection

VVA: Variable valve actuation

Table 1. Single cylinder engine specifications

Engine type	Single cylinder, 4 Stroke, DI
Bore x Stroke [mm]	123 x 152
Connecting rod length [mm]	225
Displacement [L]	1.806
Geometric compression ratio [-]	14.4:1
Bowl Type	Open crater
Number of Valves	4
IVO	375 CAD ATDC
IVC	535 CAD ATDC
EVO	147 CAD ATDC
EVC	347 CAD ATDC

Table 2. Physical and chemical properties of the fuels used in the study

	Gasoline	Diesel B7
Density [kg/m^3] (T= 15 °C)	739	837.9
Viscosity [mm^2/s] (T= 40 °C)	-	2.67
RON [-]	98.8	-
MON [-]	85.2	-
Cetane number [-]	-	54
Lower heating value [kJ/kg]	41.32	42.61

Table 3. Diesel injector characteristics

Actuation Type	Solenoid
Steady flow rate @ 100 bar [cm^3/s]	28.56
Number of Holes	7
Hole diameter [μm]	194
Included Spray Angle [°]	142

Table 4. Gasoline injector characteristics

Injector Type	Saturated
Steady flow rate @ 3 bar [cm^3/min]	980
Included Spray Angle [°]	30
Injection Pressure [bar]	5.5
Injection Strategy	Single
Start of Injection Timing	385 CAD ATDC

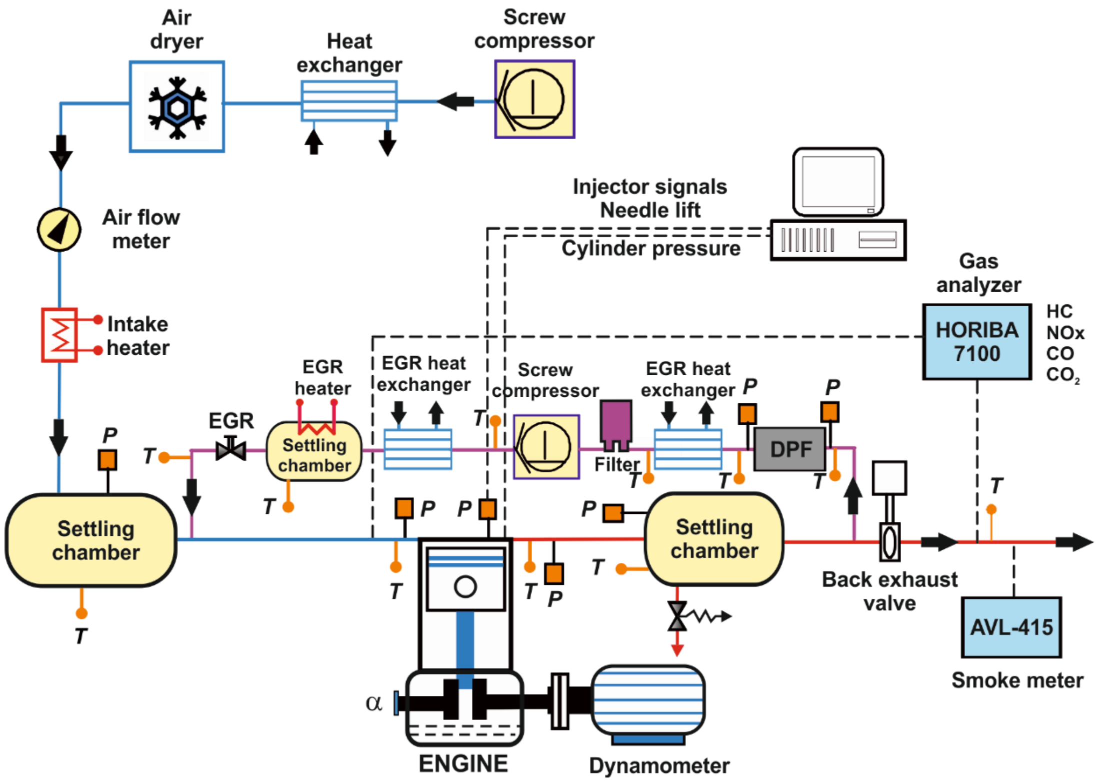

Figure 1. Complete test cell setup

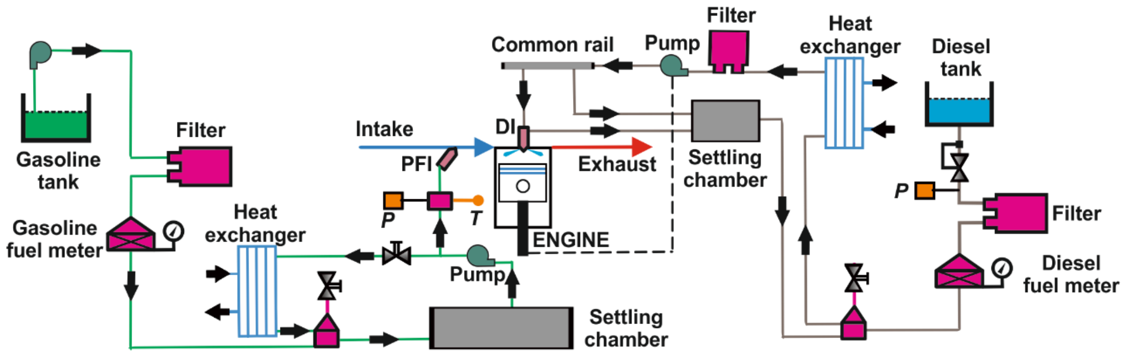

Figure 2. Fuel injection systems scheme

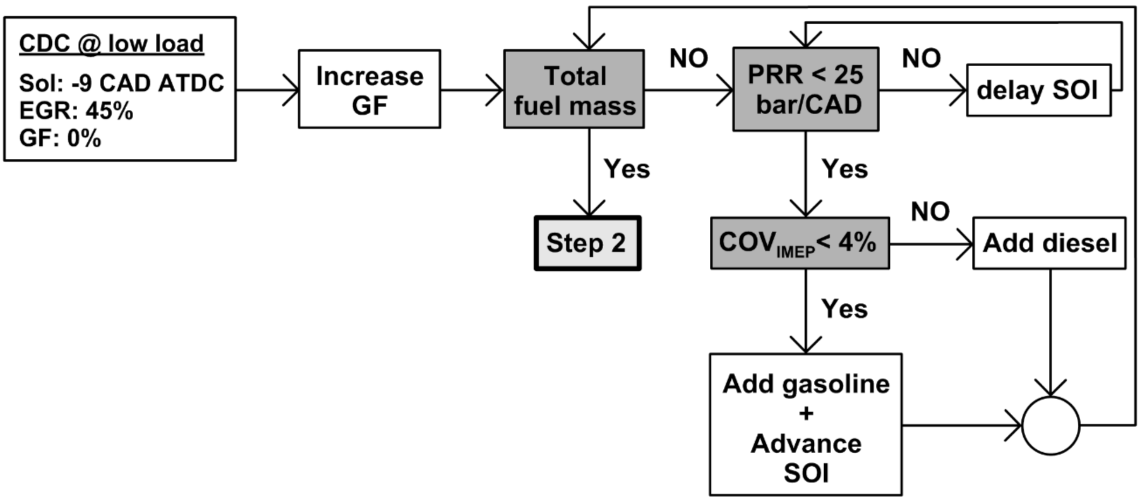

Figure 3. Experimental procedure to reach stable RCCI conditions (Step 1).

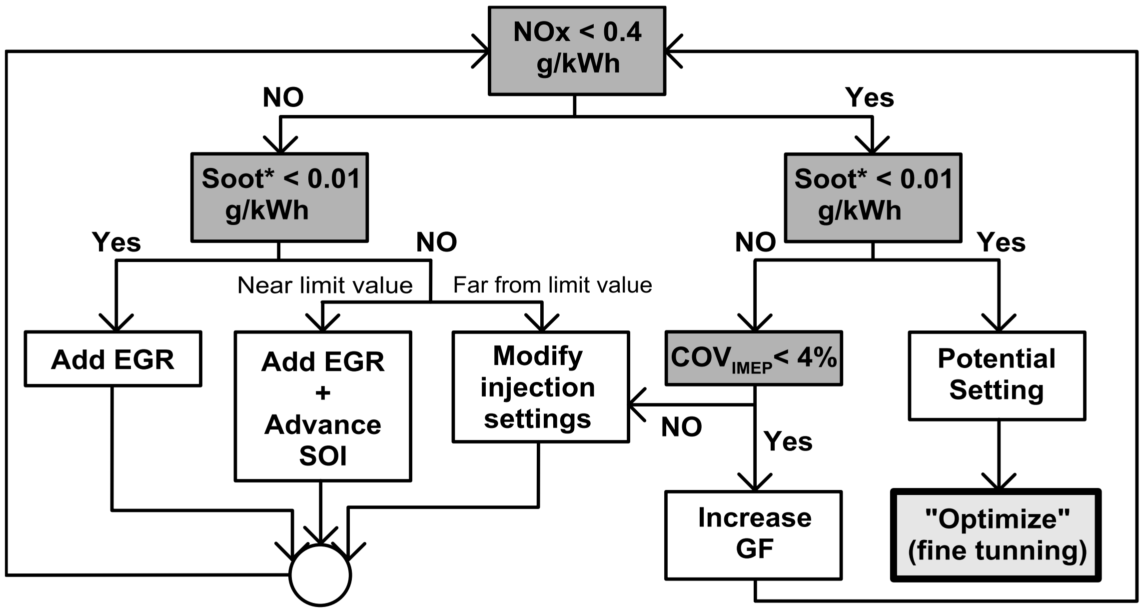

Figure 4. Experimental procedure to introduce the stable RCCI operating points from Step 1 under EURO VI NOx and soot* limits (Step 2).

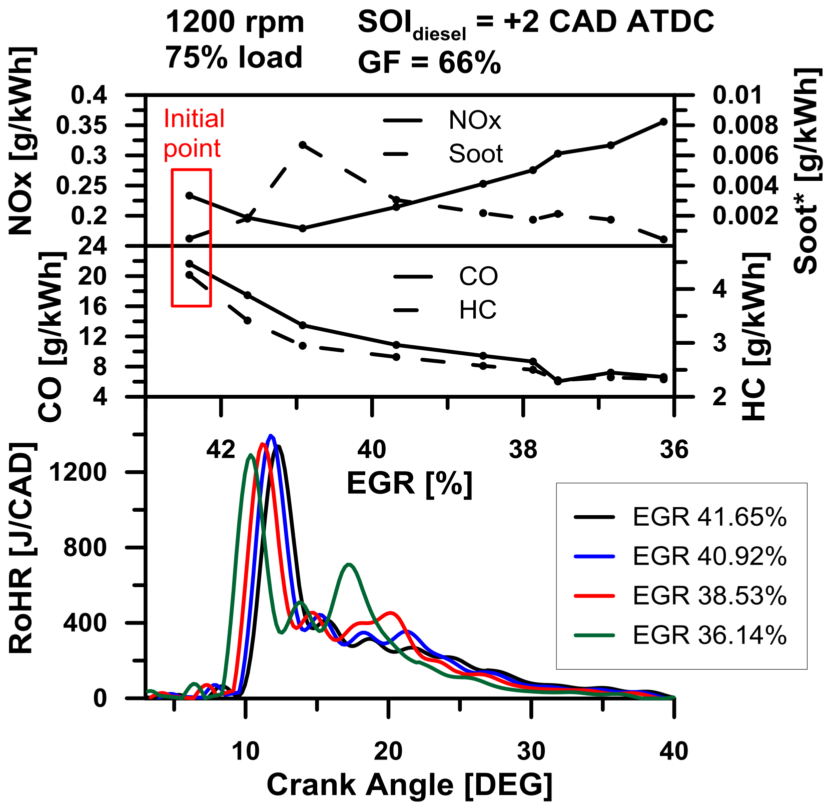

Figure 5. Effect of EGR rate on RCCI engine-out emissions at high load and 1200 rpm.

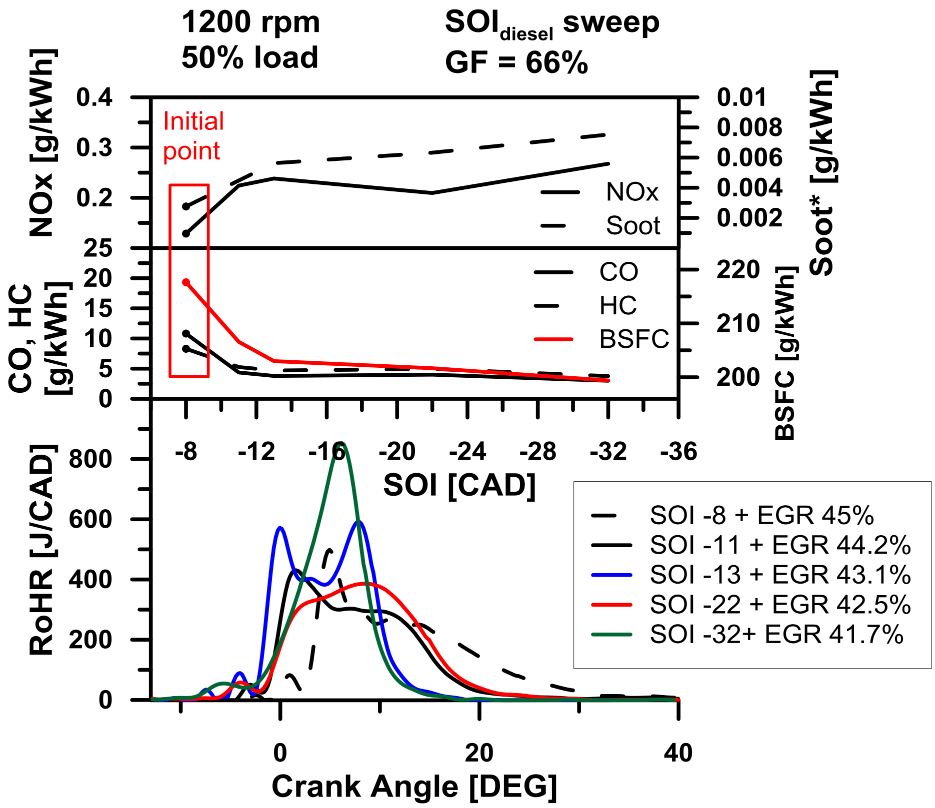

Figure 6. Effect of the combined modification of the EGR rate and diesel SOI on RCCI engine-out emissions at medium load and 1200 rpm.

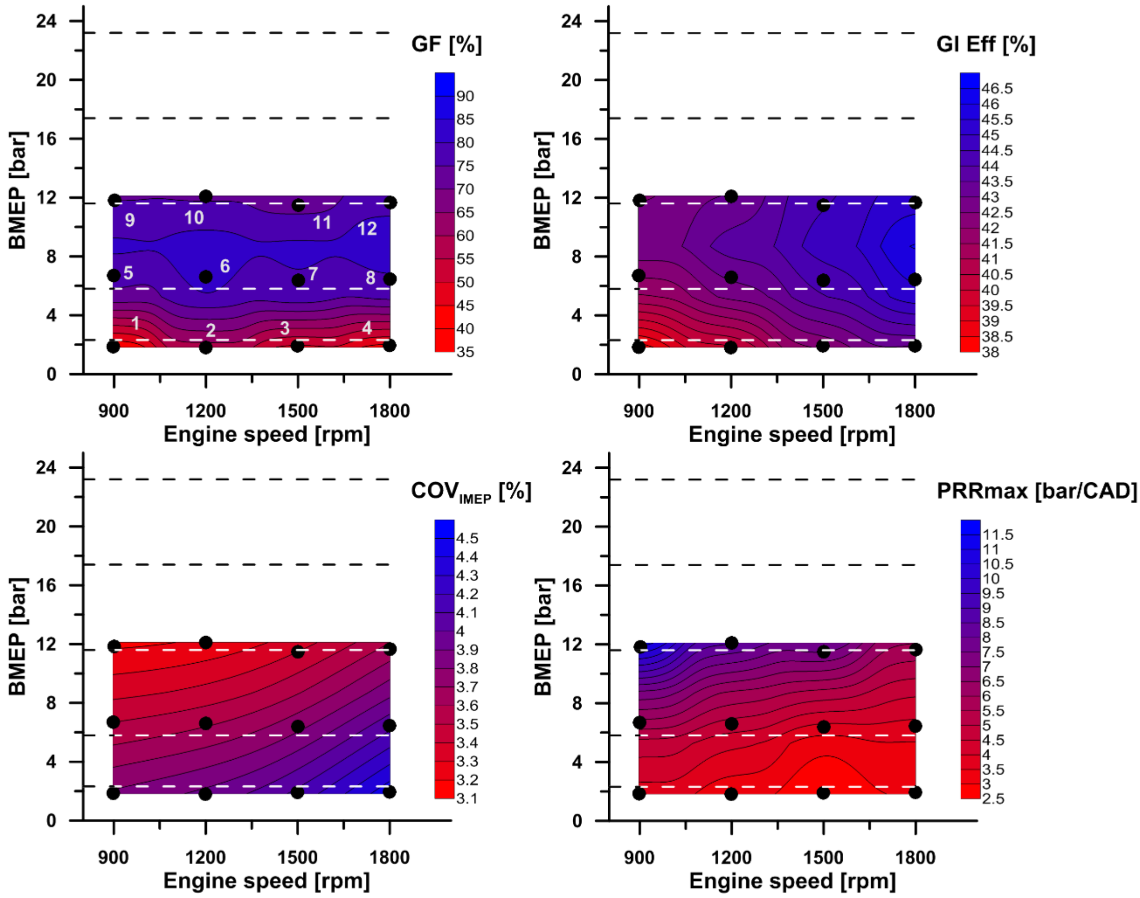

Figure 7. Different engine parameters with effective compression ratio of 14.4:1.

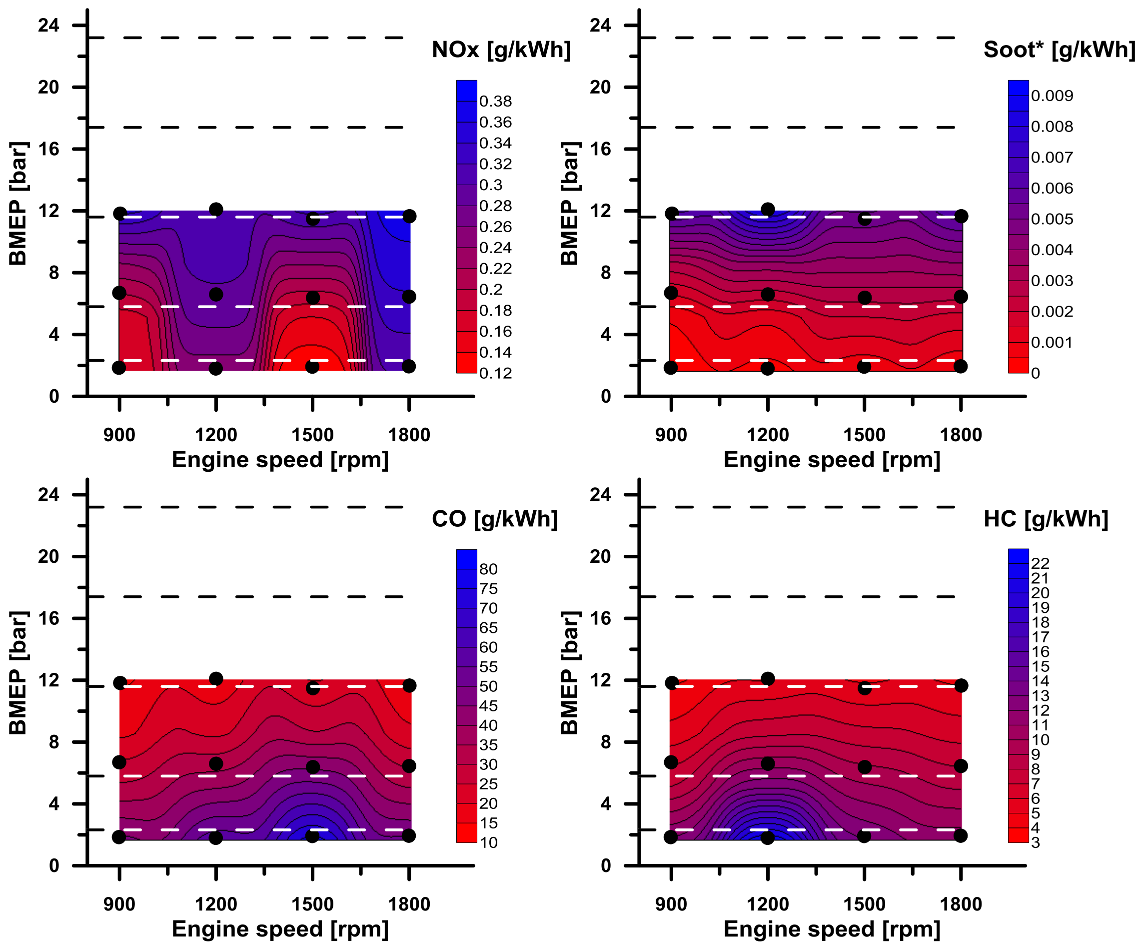

Figure 8. Engine-out emissions with nominal compression ratio of 14.4:1.

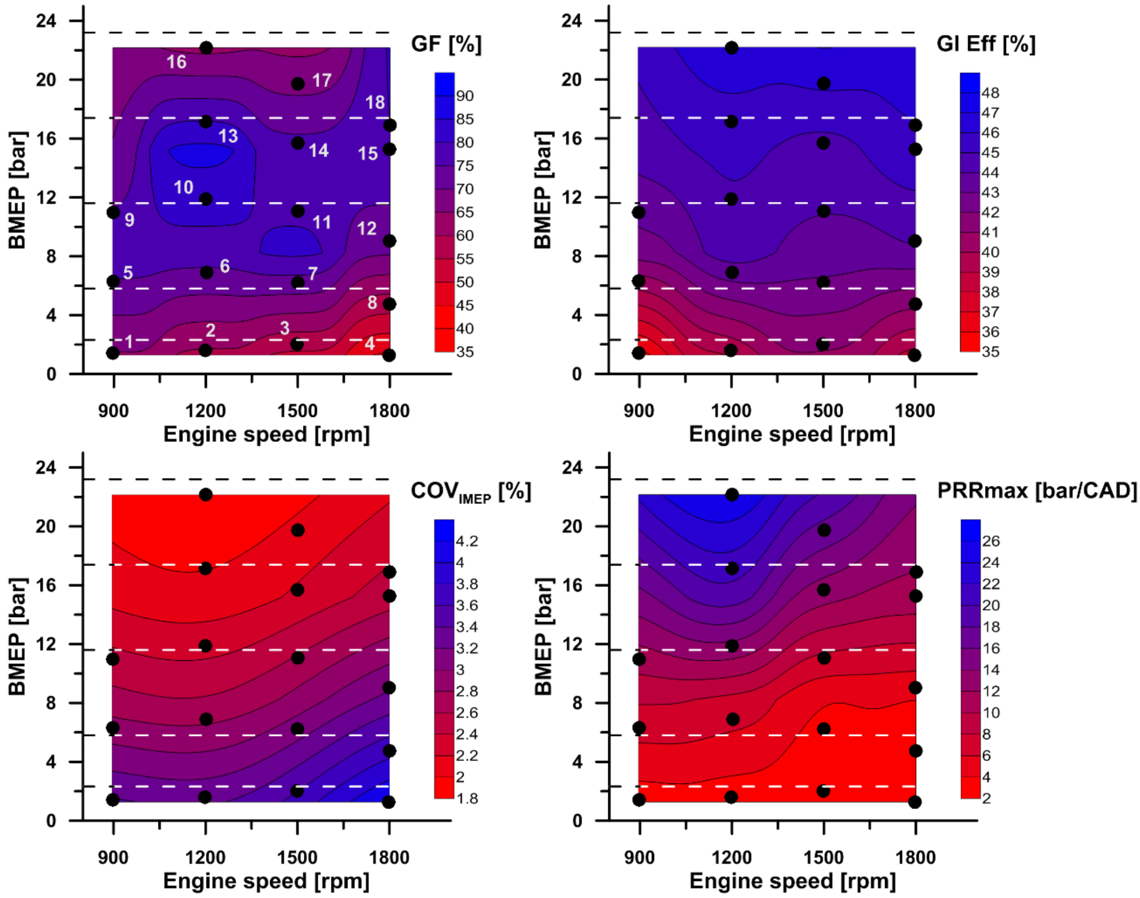

Figure 9. Different engine parameters with effective compression ratio of 11:1.

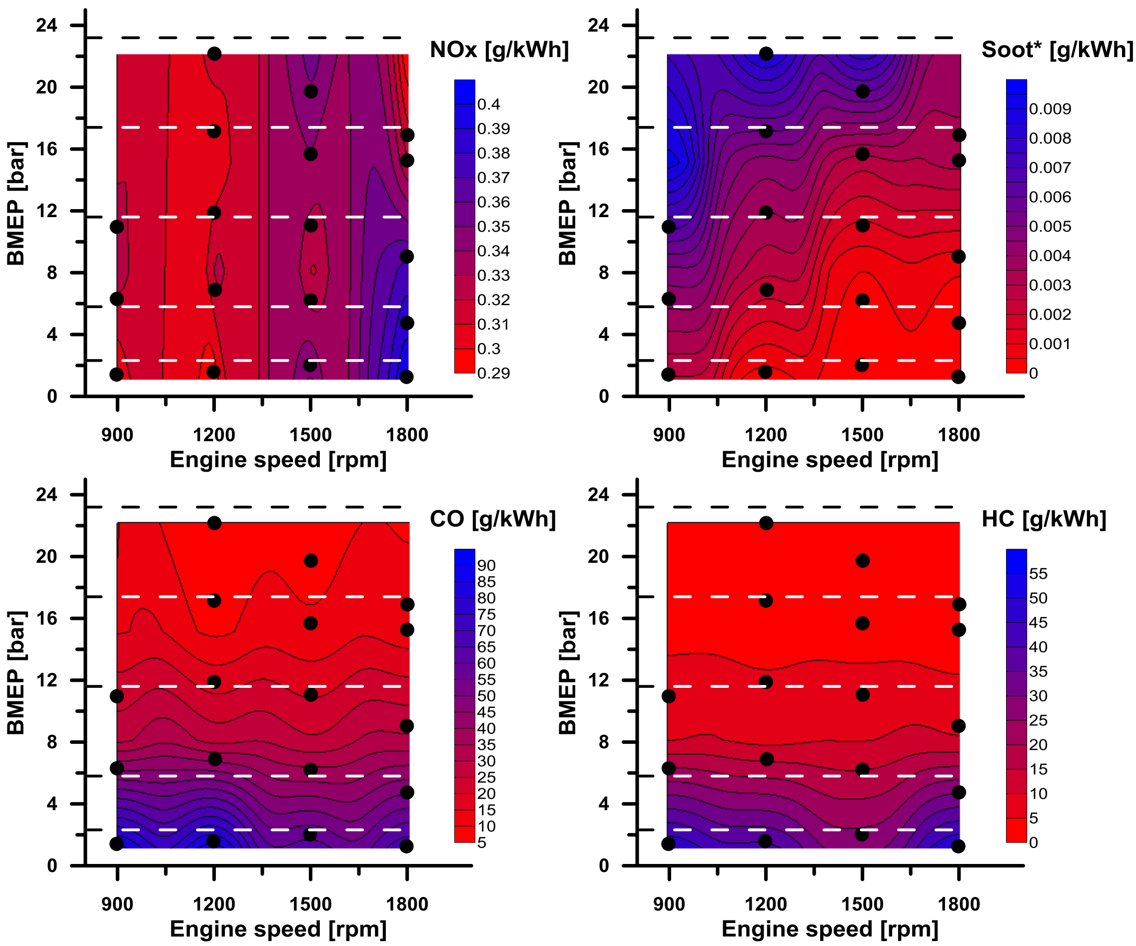

Figure 10. Engine-out emissions with effective compression ratio of 11:1.

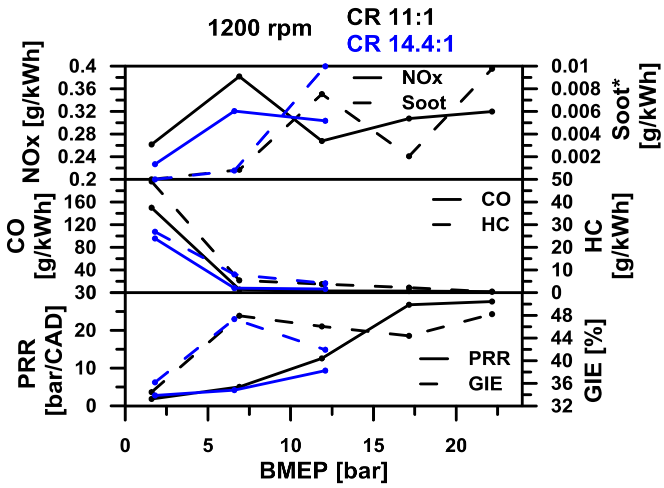

Figure 11. Engine-out emissions, PRR and GIE versus engine load for both compression ratios, 11:1 and 14.4:1 at 1200 rpm.